Numerical Simulation of Lithium-ion Battery Cooling Techniques for Electric Vehicles

Amany Belal
Arab Academy for Science and Technology and Maritime Transport, Egypt

Ali I. Shehata
Mechanical Engineering Department, College of Engineering and Technology, Arab Academy of Science, Technology and Maritime Transport, Egypt

Yehia A. Eldrainy
Mechanical Engineering Department, College of Engineering and Technology, Arab Academy of Science, Technology and Maritime Transport, Egypt

Essam H. Seddik
Mechanical Engineering Department, College of Engineering and Technology, Arab Academy of Science, Technology and Maritime Transport, Egypt

To cite this article:

Numerical Simulation of Lithium-ion Battery Cooling Techniques for Electric Vehicles

Amany Belal, Ali I. Shehata, Yehia A. Eldrainy, Essam H. Seddik

Article Info	Abstract
	Various strategies were developed for battery cooling including air cooling, liquid cooling, fin cooling, phase change material cooling (PCM), and heat pipes. The objective of this study was to identify an appropriate cooling technique for lithium-ion batteries utilized in electric vehicles. A three-dimensional unsteady numerical model was developed using ANSYS software to conduct simulations to assess the cooling efficiency of each approach. The numerical results indicate that the air-cooling technique yielded a peak temperature of 32.928 °C and a maximum total heat flow of 11456 W/m². The fin cooling technique had a peak total heat flow of 0.014476 W/m² and reached a maximum temperature of 35.17 °C. The liquid cooling technique exhibited a peak temperature of 31.773 °C and a maximum total heat flux of 10642 W/m². Additionally, a changed battery pack was planned with extra air outlets to upgrade the convection cycle of the air-cooling technique. Based on the numerical findings, the modified battery pack for air-cooling technique resulted in a peak temperature of 31.214 °C and a maximum total heat flow of 12272 W/m². PCM and heat pipe method had a maximum temperature of 54.85 °C and a maximum total heat flow of 554.69 W/m². According to the results obtained, the liquid cooling method demonstrated the lowest maximum temperature. The simulations indicate that this approach offers the most effective thermal management, with a maximum temperature value of 31.773 °C.

Introduction

Using a lithium-ion battery in automobiles eliminates fuel consumption and reduces carbon dioxide emissions, which has significant environmental benefits. The demand for lightweight and compact power sources led to the emergence of lithium-ion batteries. Lithium-ion batteries are popular for electric vehicles due to their high energy density, low self-discharge, long life, and stability. However, battery life and security can become compromised as battery volumes decrease and power increases. To address this, developing proprietary lithium-ion battery thermal management systems is crucial, as their performance, durability, and safety are significantly influenced by cell temperature (Lu et al., 2013).

Cooling is vital for lithium-ion battery thermal management, particularly compared to lead-acid, Ni-MH, and sodium Sulphur batteries (Omariba et al., 2020). This is due to the heat generated during regular battery use, which must be dissipated to prevent the battery from reaching a specific threshold temperature (around 40 °C) (Bandhauer et al., 2011) and possibly activating the thermal runaway process [3,4], which can lead to a catastrophic battery fire (Bandhauer et al., 2011) if the cell temperature reaches 80–100 C. Lithium-ion (Li-ion) battery cooling aims to maintain the temperature of the batteries below a certain threshold (roughly 40 °C) and achieve uniform temperature distributions for each cell and within the battery pack under demanding operating conditions [5]. This is accomplished by slowing or suppressing the battery's rapid temperature rise under adverse circumstances, such as an external short (Wang et al., 2012, Feng et al., 2012, Abaza et al., 2018, Zhao et al., 2015). The ideal working temperature range is between 20 and 40 °C, and the temperature differential within a battery pack should be kept to no more than 5 degrees (Qian et al., 2016, Rao & Zhang, 2019).

The charging and discharging process of lithium-ion batteries necessitates a heat management system. Liquid cooling, heat pipe cooling, air cooling, and cooling with phase change materials are among the thermal management strategies explored for lithium-ion batteries (Ramadass et al., 2002, Liu et al., 2017). Liquid cooling has been found to have greater heat exchange efficiency and better temperature management. Air (Park, 2013, Yu et al., 2019) and mini-channel plate liquid cooling (Wei & Agelin-Chaab, 2018, Menale et al., 2019) are the most used lithium battery cooling techniques. PCM cooling (Bai et al., 2017), heat pipe cooling (Tran et al., 2014), direct liquid cooling (single-phase) (Deng et al., 2018), and direct liquid cooling (two-phase) (Wang & Wu et al., 2020) are other cooling strategies. The most critical factors in preserving a Li-Ion battery's health, life, and safety are a dynamic measurement of the accurate and reliable state of charge (SOC) (Zhou et al., 2017) and an effective battery thermal management system (BTMS) (Liu et al., 2017, Kim et al., 2019).

High and low temperatures impact a lithium-ion battery's performance negatively. Operating below the optimal operating temperature affects energy yields, and the most significant power while operating above the optimal operating temperature can lead to safety and aging issues. During battery charging and discharging, internal heat is generated, resulting in higher temperatures (Liu et al., 2014), which can lead to thermal runaway and an internal short circuit. Thermal runaway can cause fire and explosion in extreme cases (Ismail et al., 2013).

Heat formation in a lithium-ion battery is caused by changes in enthalpy, electrochemical polarization, Joule heating, and resistive heating (Ismail et al., 2013). Batteries typically reach temperatures of up to 55 °C (Duan et al., 2014). Energy capacity and cycle life are impacted when temperatures are below 0 °C and above 40 °C (Saw et al., 2015) The optimal operating temperature range for a lithium-ion battery is between 25 and 40 °C (Liu et al., 2015), with the ideal temperature range for a battery pack being 3 to 5 °C and 5 to 10 °C for a battery cell (Saw et al., 2015).

Manufacturers use various cooling administration strategies to reduce heat generated in the lithium-ion battery, including air, fin, and liquid cooling (Mousavi et al., 2011). Pesaran (199) proposed the air-cooling thermal management design, in which the low energy density air-cooling method is studied, and the problems with using air as a cooling medium in battery modules are noted.

Phase change material (PCM) has been the subject of many studies on low thermal conductivity (Choudhari et al., 2020) and leakage difficulties (Lv et al., 2017) since it was first employed to manage lithium-ion batteries in 2000 (Al Hallaj & Selman, 2000). Heat storage systems frequently use heat pipe technology, which operates on evaporative heat transmission. Wu *et al*., (2002) in their initial study of the thermal dissipation system of the lithium-ion battery based on the heat pipe technology in 2002, found that the heat pipe cooling technique can bring the battery's surface temperature down to about 32 °C. Fins were introduced to increase the temperature uniformity when using air cooling, and their performance has improved (Tran et al., 2014). Temperature homogeneity was improved by using a metal foam in the air channel and fin pins (Mohammadian et al., 2015; Mohammadian & Zhang, 2015).

The most critical details in this text are that low discharge rates were used for all these tests and that PCM-graphite composites were introduced to improve the thermal conductivity temperatures (Sabbah et al., 2008; Ling et al., 2014). Copper and aluminum were used as test metals for metal foam made with pure PCM (Li et al., 2014; Wang et al., 2015). Compared to cylindrical and prismatic cells, Z-fold pouch cells have demonstrated more excellent heat dissipation and, as a result, a high performance (Kokam, 2016). The thermal conductivity is lower in the direction of thickness and higher in the direction of length and width for prismatic and pouch cells, respectively. Therefore, for better temperature distribution, the cooling should be done in the direction of length and width (Chen & James, 1994).

Air cooling is one of the warm administration strategies producers utilize to decrease heat created in the lithium-ion battery. Holes between cells in a battery pack permit space for air to go through and assimilate heat through convection. A centrifugal fan pumps outside air into the battery pack when the vehicle is moving (Hwang et al., 2014). Yaojuan Duan from Beijing Jiaotong College directed an ANSYS simulation to look at temperature circulations of a battery pack with and without air cooling. His simulation brought about a last surface temperature of roughly 49 °C without cooling and 37 °C with cooling. Hsiu-Ying Hwang of the National Taipei University of Technology also developed a computational fluid dynamics model to simulate airflow conditions. Hwang's model diminished heat in the battery pack by 39% moving (Chen et al., 2016). Liquid cooling is a technique used by producers to move intensity from the lithium-ion battery. It can be divided into two categories: direct and indirect. However, due to the potential for leaks discovered in previous studies, the indirect liquid cooling method needs to be considered for the calculation moving (Chen et al., 2016). Indirect liquid cooling involves a jacket containing a coolant that wraps around the battery and circles the coolant by a pump moving (Chen et al., 2016). Direct liquid cooling involves spraying a liquid over the battery pack to facilitate convection-based heat transfer. Shiraz University researcher Gholamreza Karimi investigated the effects of dielectric silicone oil as a liquid cooling fluid. His research demonstrated that the oil increased the system's heat removal and that, due to the fluid's high heat capacity, liquid cooling is more efficient than air cooling moving (Karimi & Li., 2012).

Fin cooling is a strategy for heat decrease of a battery, using a rectangular metal block attached to the battery pack. The fin's material has a high thermal conductivity, allowing it to conduct heat from the battery. Dafen Chen carried out a study from the National Renewable Energy Laboratory of Colorado to understand the effects of air, fin, and

liquid cooling on a lithium-ion battery. His fin cooling simulation on ANSYS used an aluminum fin with dimensions of 169 mm x 197 mm x 1 mm and a thermal conductivity of 202.4 W/mk [43]. Air and liquid cooling were more effective than the fin in thermal management because they provided an ideal battery operation temperature below 40 °C (Liu et al.., 2015). The target of this paper was to investigate the impacts of each kind of technique for heat transfer inside lithium-ion batteries.

Method

Physical Domain

To compare the different methods of battery cooling, a physical domain of the battery pack with a dimension of 500 x 300 x 200 mm was used, (see Figure 1). The opening at the top of the battery pack is an inlet flow with different convection heat transfer coefficients, and the opening at the bottom-right of the pack is an outlet of the warm flow. ANSYS numerical simulation-based software was used to obtain the temperature gradients and average temperature for each cooling method. Air and dielectric mineral oil serve as the working fluid for the forced convection cooling methods applied on a domain (a) (see Figure 1). Because a fan or a pump moves the working fluid across the battery pack, forced convection with a different heat transfer rate can be adopted according to the following equation:

$$Q_{conv} = A_s\, h\, (T_s - T_\infty) \tag{1}$$

where (A_s) is the surface area, h is the heat transfer coefficient, and T_s and T_∞ are temperatures of the wall surface and the ambient air, respectively. The heat transfer coefficient of the air is assumed to be between 100 and 1000 W/m²K, while the heat transfer coefficient of dielectric mineral oil is assumed to be 1200 W/m² K. Air temperature (20 °C) was assumed for the air and liquid.

The third cooling method is conduction-dependent, using fin cooling applied on domain (b) (see Figure 1). The battery pack had a fin-like aluminum plate attached to one side. The aluminum plate's high thermal conductivity absorbed the battery pack heat through direct contact. The conduction equation is:

$$Q_{cond} = \frac{A\,k\,(T_1 - T_2)}{L} \tag{2}$$

Where (A) is the fin area. The fin thermal conductivity is represented by (K). The battery pack temperature is (T_1). The temperature of the fin is (T_2). The fin length is (L).

Given that the fin tip is air-cooled, the condition at the tip is convection heat transfer. The temperature dissemination condition is:

$$\frac{T(x) - T\infty}{Tb - T\infty} = \frac{\cosh m(L-x) + (h/mk)\sinh m(L-x)}{\cosh mL + (h/mk)\sinh mL} \tag{3}$$

The heat rate equation for the fin is:

$$Q_{f} = M\, \frac{\sinh mL + (h/mk)\cosh mL}{\cosh mL + (h/mk)\sinh mL} \tag{4}$$

Condition 3 was utilized for ascertaining the intensity move rate from the battery pack to the blade. Like the study by Dafen Chen discussed before, this method made it possible to calculate the fin at a predetermined temperature of 20 °C. The aluminum fin is attached to the proper attachment, and the opening at the top serves as an air inlet and outlet. It is made of 6061 alloys and has a thermal conductivity of 173 W/m K.

The Steady-State Thermal procedure determined an initial temperature of 22 °C, which was uniform and applied to the entire geometry. The model's internal heat generation was used to represent the battery's charging and discharging heat, with a rate of 1.0092 e+5 W/m^3 with a volume of 0.012 m^3 and a heat rate of 1,211 Watts. The geometry's inlet and fin were subjected to convection, with a film coefficient of 1000 W/m^2°C and a temperature of 20 °C, indicating that air was applied consistently across the battery pack and fin. For the water cooling, the internal heat generation rate was 1.1667e+5 W/m^3 (3,500 Watts/0.03m^3) with a heat rate of 3,500 Watts. The geometry's inlet was subjected to convection, and the dielectric mineral oil had a film coefficient of 1200 W/m^2°C at 20 °C. This procedure assumes that the liquid was evenly applied to the inside walls and top of the battery pack.

Illustrative Equations for PCM

The continuity, momentum, and energy equations for the thermal response of the PCM are classified as follows:

$$\frac{\partial u_r}{\partial r} + \frac{u_r}{r} + \frac{\partial u_z}{\partial z} = 0$$

$$\frac{\partial u_r}{\partial t} + u_r\frac{\partial u_r}{\partial r} + u_z\frac{\partial u_z}{\partial z} = -\frac{1}{\rho}\frac{\partial p}{\partial r} + \nu\left(\frac{\partial^2 u_r}{\partial r^2} + \frac{1}{r}\frac{\partial u_r}{\partial r} - \frac{u_r}{r^2} + \frac{\partial^2 u_r}{\partial z^2}\right)$$

$$\frac{\partial u_z}{\partial t} + u_r\frac{\partial u_z}{\partial r} + u_z\frac{\partial u_z}{\partial z} = -\frac{1}{\rho}\frac{\partial p}{\partial z} + \nu\left(\frac{\partial^2 u_z}{\partial r^2} + \frac{1}{r}\frac{\partial u_z}{\partial r} - \frac{u_r}{r^2} + \frac{\partial^2 u_z}{\partial z^2} + g[\beta(T - T_m) - 1\,]\right)$$

$$\frac{\partial h}{\partial t} + u_r\frac{\partial h}{\partial r} + u_z\frac{\partial h}{\partial z} = \frac{1}{\rho}\left[\frac{1}{r}\frac{\partial}{\partial r}\left(kr\frac{\partial T}{\partial r}\right) + \frac{\partial}{\partial z}\left(k\frac{\partial T}{\partial z}\right)\right]$$

The scaled temperature can be clarified as T_1 as an initial temperature, T_m as a melting temperature T_2 as a final temperature ($T_2 = T_m + \Delta T$). A transition happens between the solid and liquid phases during the implementation of this function within the interval of ΔT. A mushy phase also existed within the interval. It can be seen with mixed properties of the material.

T* $\leqslant$ T$_1$ (Solid phase)
T$_1$ $<$ T* $<$ T$_2$ (Mushy phase)
T* $\geqslant$ T$_2$ (Liquid phase)

(a)

(b)

(c)

(d)
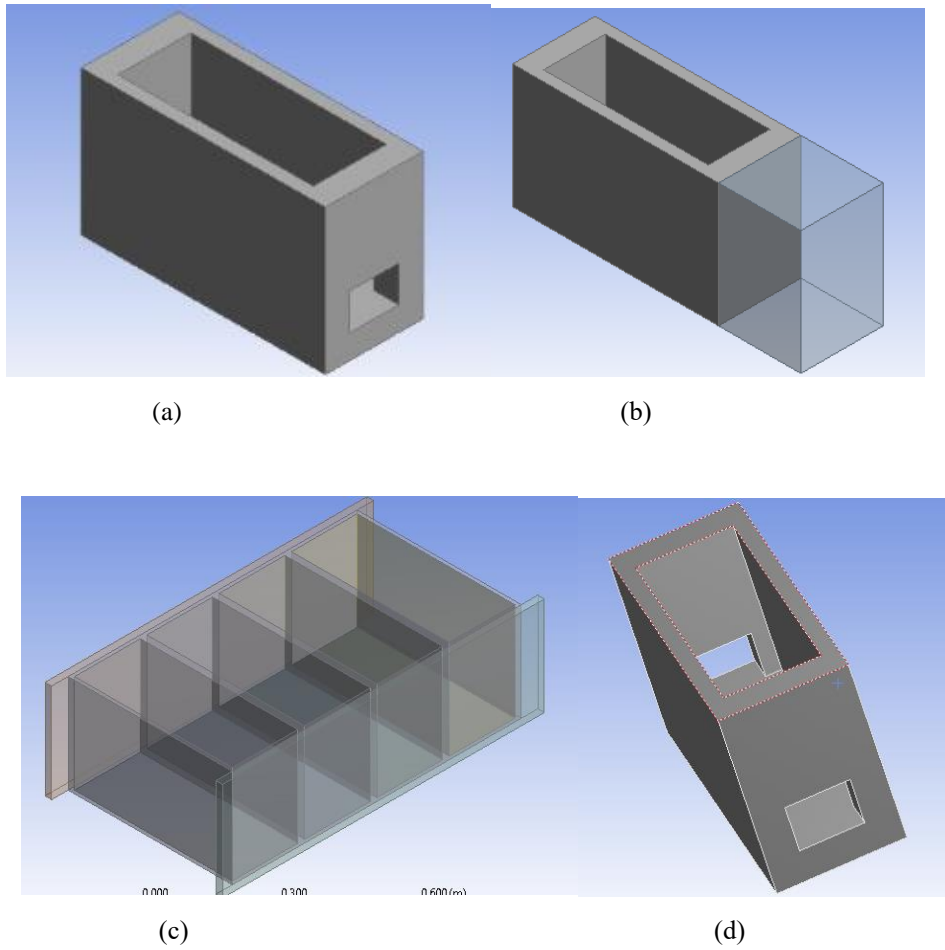
Figure 1. Battery Pack Physical Domain (A) Without Fins (B) With Fins
(C) Pcm With Heat Pipe (D) Modified Battery Pack

Mesh Generation

The meshing creation is essential to evenly distribute heat generation and convection throughout the simulation and to get accurate results. It divides the geometry into sections to ensure even distribution.
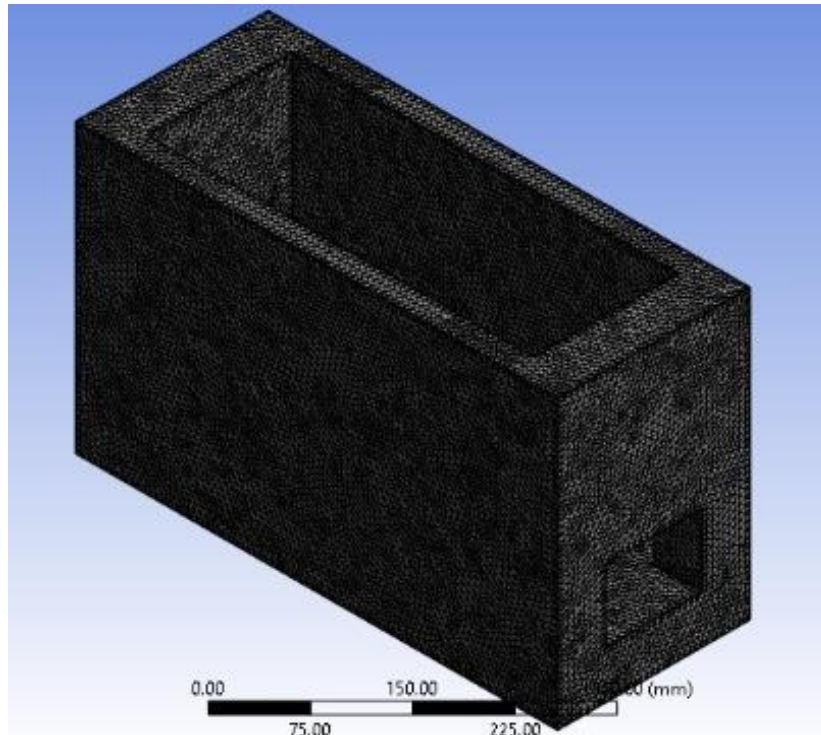
Figure 2. Meshing of Air-Cooling Model

Grid Independence Study

For the purpose of simulating the battery and airflow, the unstructured non-uniform grid is utilized in this paper. Figure 2 depicts the computational and physical domains. A non-uniform grid, in which the grid concentration is higher in some areas, is used to accurately model the battery's boundary layer and reduce computational time. A lot of calculations are done to ensure that the accuracy of the results is independent of the grid. Eventually, a grid with 172043 elements was chosen. To assess the independence of the grid solution, the number of components was varied. Table 1 presents the maximum and minimum, average temperatures for four different grids. The findings indicate that when the grid becomes finer than the one with 172043 elements, the results do not change significantly. Consequently, grid 2 is selected to reduce computational costs.

Table 1. Grid Study Using Different Grid Resolutions.

Mesh Size of Liquid	Grid 1 2 mm	Grid 2 3 mm	Grid 3 4 mm	Grid 4 5 mm
Maximum	31.775 °C	31.775 °C	31.775 °C	31.774 °C
Minimum	21.391 °C	21.39 °C	21.39 °C	21.388 °C

Average	24.702 °C	24.706 °C	24.727 °C	24.746 °C

Results

Air Cooling

Figures 3 and 4 depict the selected case's temperature distribution at discharge's conclusion. demonstrate the effects of air cooling. The temperature gradually rises from the inlet to the outlet in air cooling. Because heat conduction is slower in the bottom layer than in the upper layers, the bottom layer is hotter than the upper layers. Due to the relatively low thermal conductive coefficient of air, shown by the temperature at the edge of the inlet side, the temperature difference between the surface of the battery pack and the coolant in air cooling is more significant than in liquid cooling.

The system's average temperature was 26.311 °C, and after 600 seconds, it reached a minimum temperature of 21.754 °C. This temperature was seen closer to the geometry's upper layers, where convection was at its greatest. The geometry's bottom layer experienced the highest temperature at 32.928 °C, as the battery pack's bottom received the lowest cooling airflow. These results are equivalent to Yaojuan Duan's concentrate, and Duan's study also produced similar temperature contours for his ANSYS air cooling model. These results are supported by the fact that the temperatures at their lowest and highest points were comparable. The Total Heat Flux simulation showed that the minimum heat flux was 4.3157e-10 W/m^2, the maximum was 11456 W/m^2, and the average was 3141.5 W/m^2. A 600-second simulation was used to determine these findings.
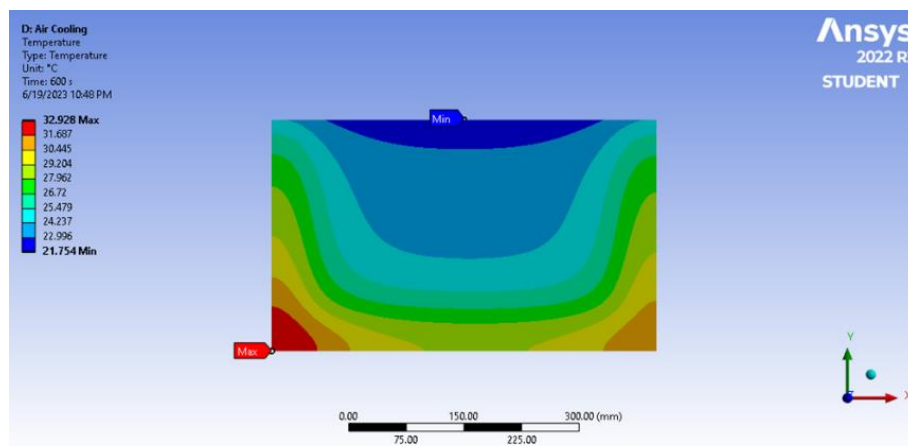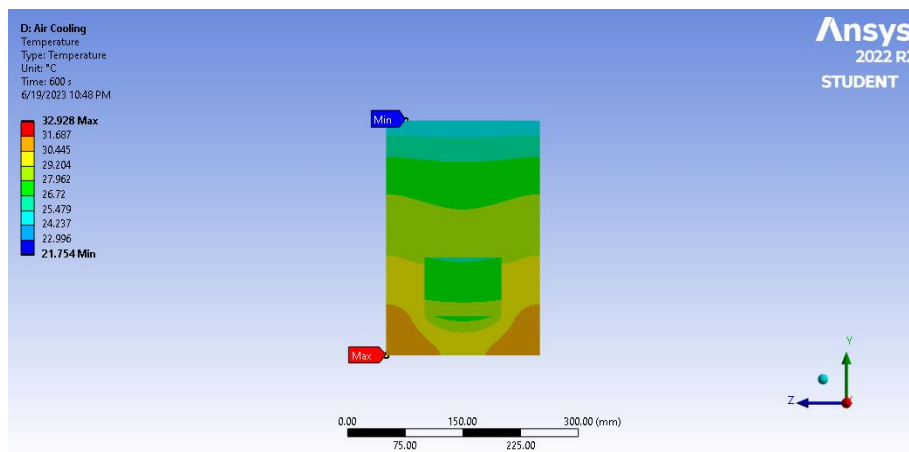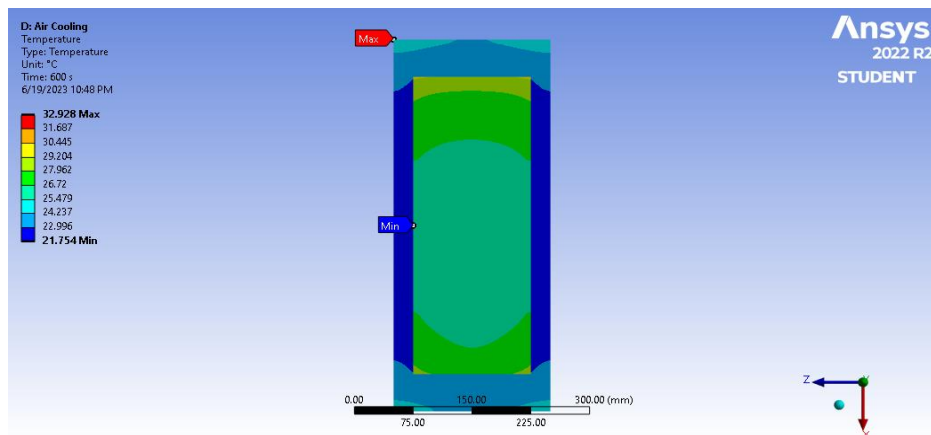
Figure 3. Temperature Solution of Air Cooling
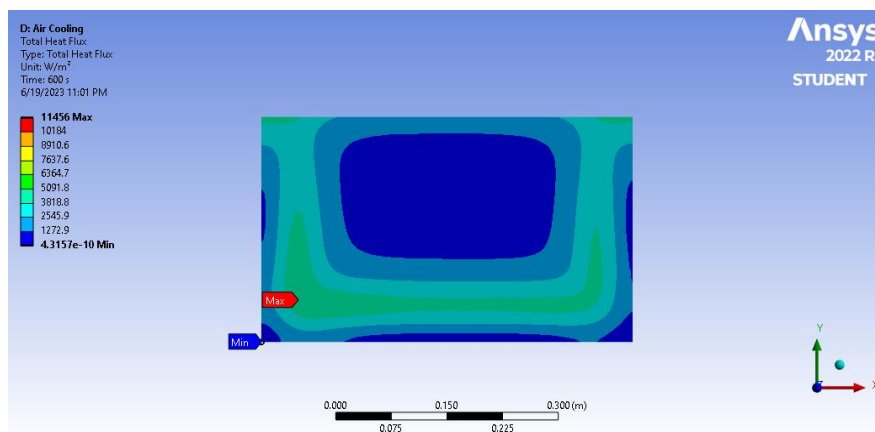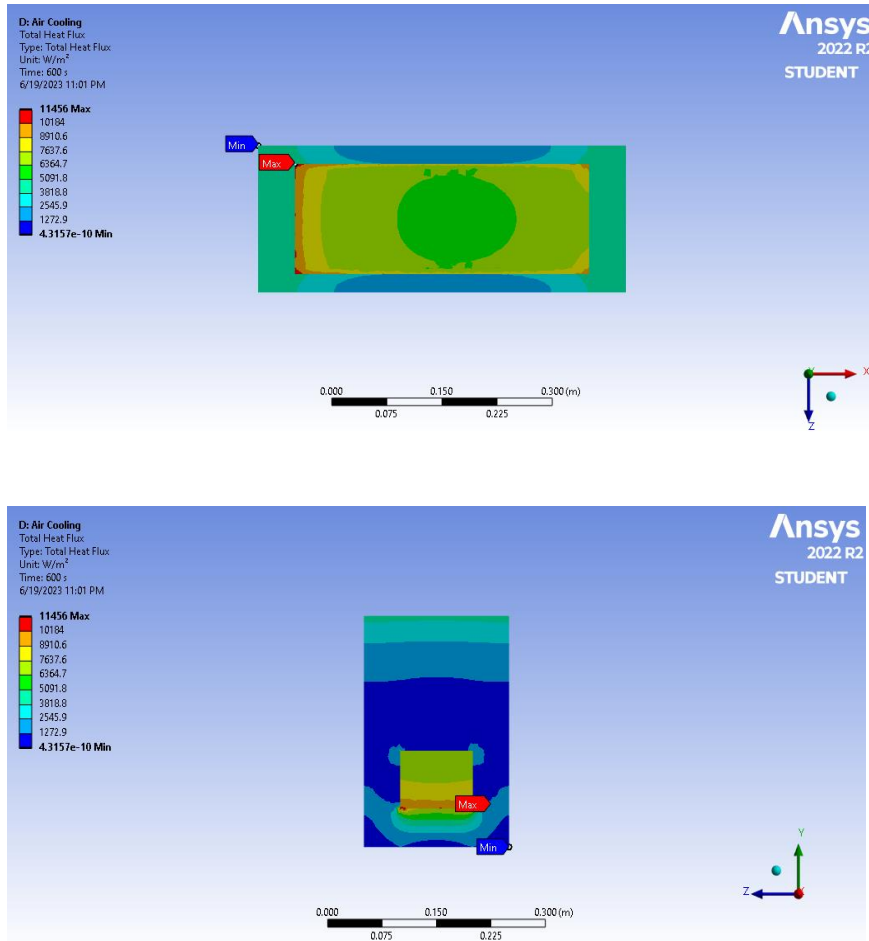
Figure 4. Total Heat Flux Solution of Air Cooling

Fin Cooling

Figures 5 and 6 depict the selected case's temperature distribution at discharge's conclusion. and demonstrate the effects of fin cooling. The system's average temperature was 23.499 °C, and after 600 seconds, it reached a minimum temperature of 20.09 °C. This temperature was observed when direct convection was applied to most of the fin's surface. The geometry's bottom layer experienced the highest temperature at 35.17 °C, which is expected due to the enclosed geometry resulting in the most significant production of internal heat at the bottom. Heat uniformity was shown by the temperature contour (see Figures 5,6) on the battery pack's longer side. These outcomes are comparable to Dafen Chen's study, which utilized an aluminum fin. Even though the fin in this simulation is more significant to allow for maximum heat transfer, Chen's research also demonstrated that the fin maintained a uniform temperature. The Total Heat Flux simulation showed that the minimum heat flux was 9.2212e-8 W/m², the maximum was 0.014476 W/m², and the average was 2379.7 W/m². A 600-second simulation served as the basis for these findings.
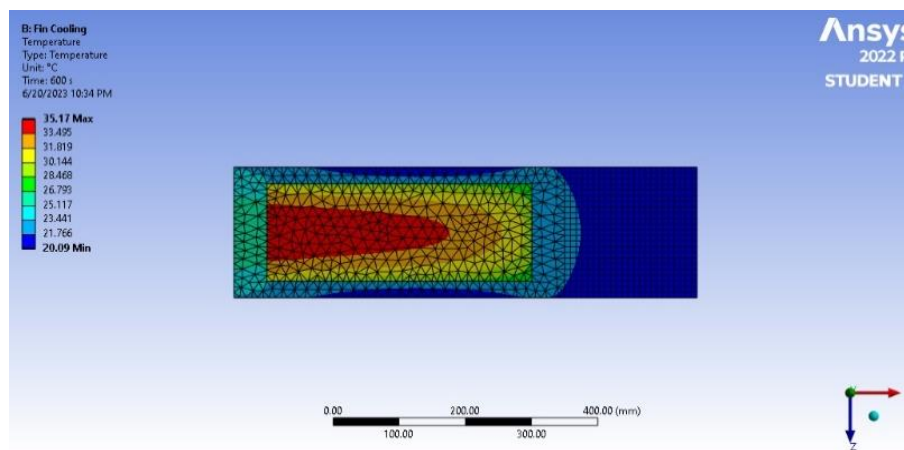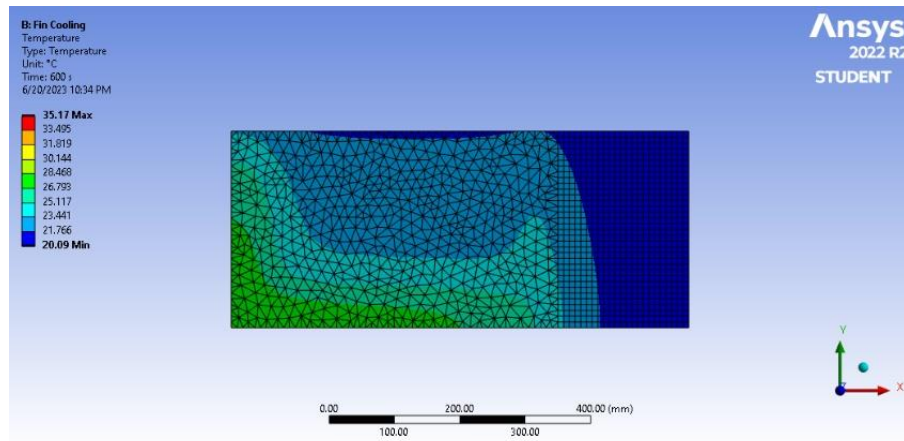
Figure 5. Temperature Solution of Fin Cooling
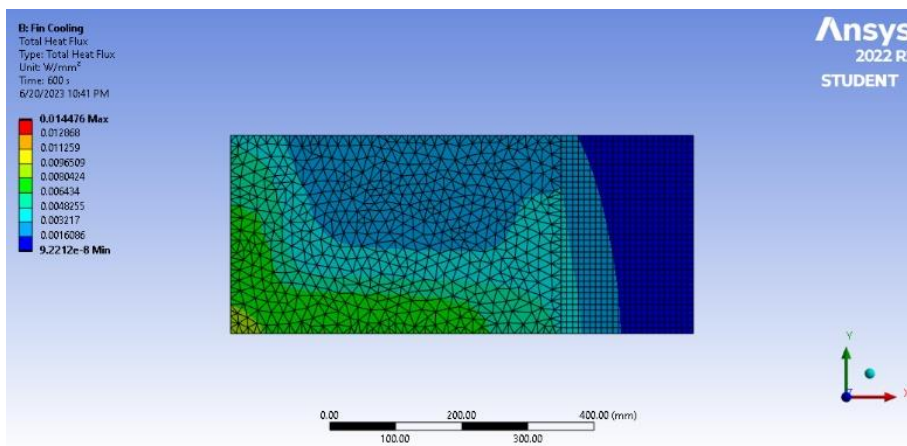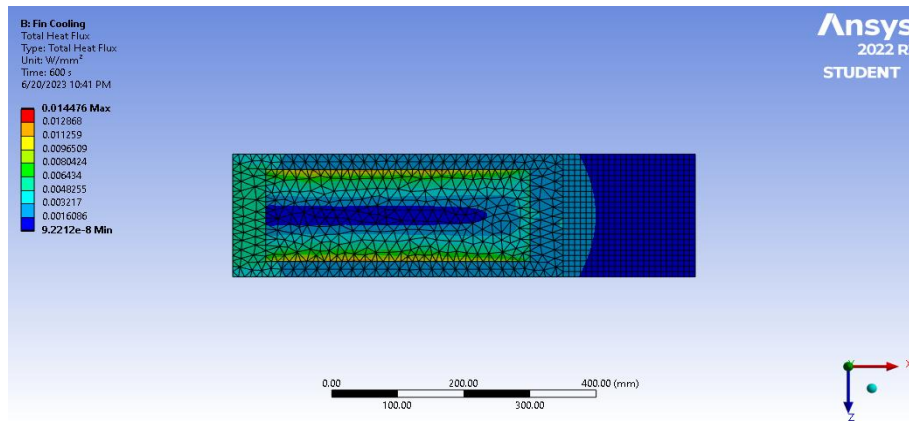
Figure 6. Total Heat Flux Solution of Fin Cooling

Liquid Cooling

Figures 7 and 8 provide visual representations of temperature distribution in the selected case, specifically focusing on the impact of cooling methods on liquids. Direct liquid cooling causes a gradual temperature increase from the inlet to the outlet. However, due to slower heat conduction in the bottom layer compared to the upper layers, the bottom layer tends to be hotter. When comparing liquid cooling to air cooling, air cooling exhibits a greater temperature difference between the battery pack's surface and the coolant. This is attributed to the relatively low thermal conductive coefficient of air. Although direct liquid cooling has a more significant effect on battery temperature, its temperature distribution resembles that of air cooling, resulting in a larger temperature angle.

During a 600-second simulation, the average temperature of the framework was 24.746 °C, with the lowest temperature recorded at 21.386 °C. The highest temperature was observed in the bottom layer of the enclosed geometry, reaching 31.773 °C. This is expected as the bottom layer generates the most internal heat. The temperature contour in Figures 7, 8 indicates that the longer side of the battery pack experiences uniform heating. These findings align with a previous study by Gholamreza Karimi, which used dielectric silicone oil with a high heat capacity at a temperature of 20 °C. Regarding the Total Heat Flux simulation, the minimum heat flux was measured at 0.020655 W/m^2, while the maximum intensity motion reached 10642 W/m^2. The average heat flux was calculated as 2873.5 W/m^2. These values were obtained from a 600-second simulation.
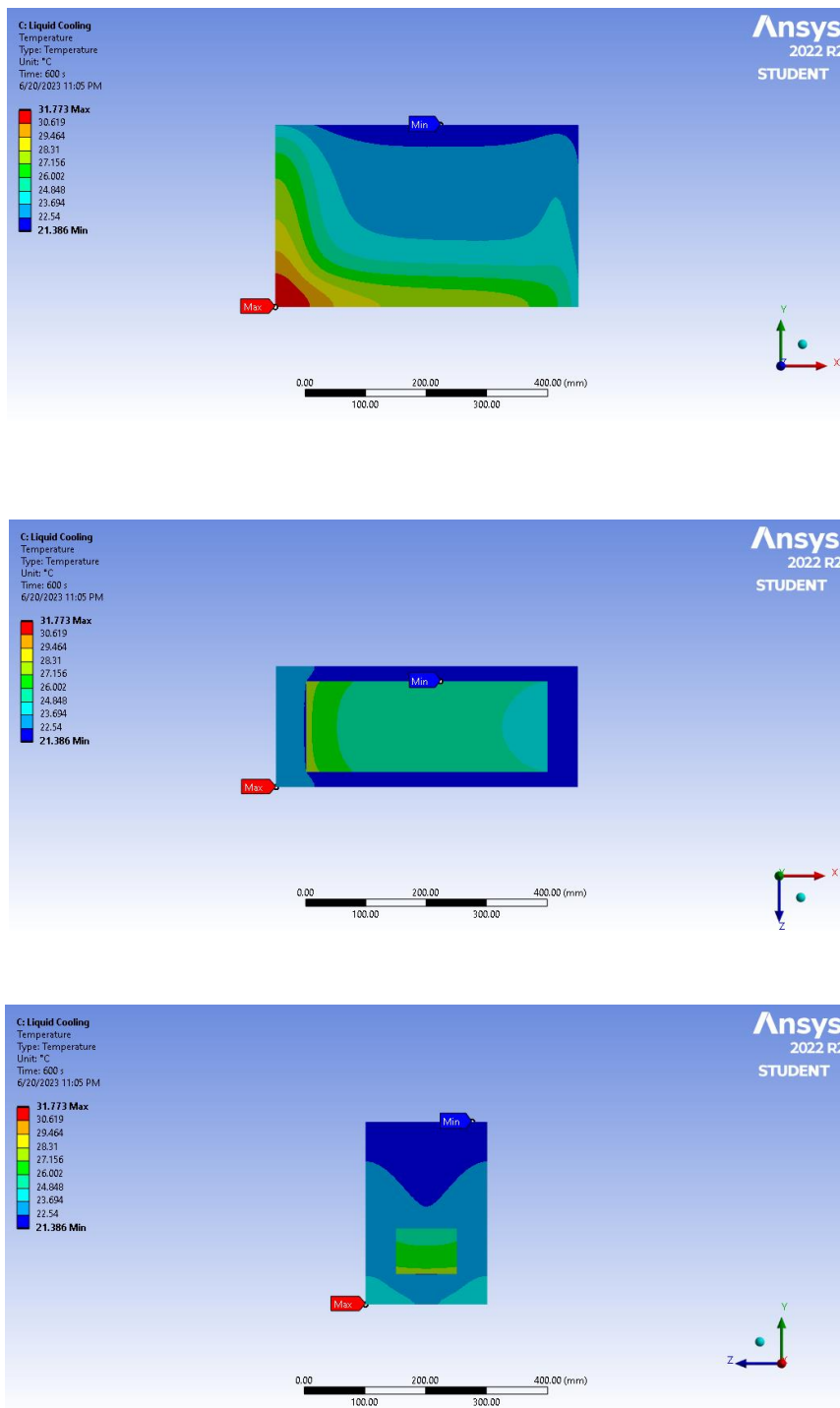
Figure 7. Temperature Solution of Liquid Cooling
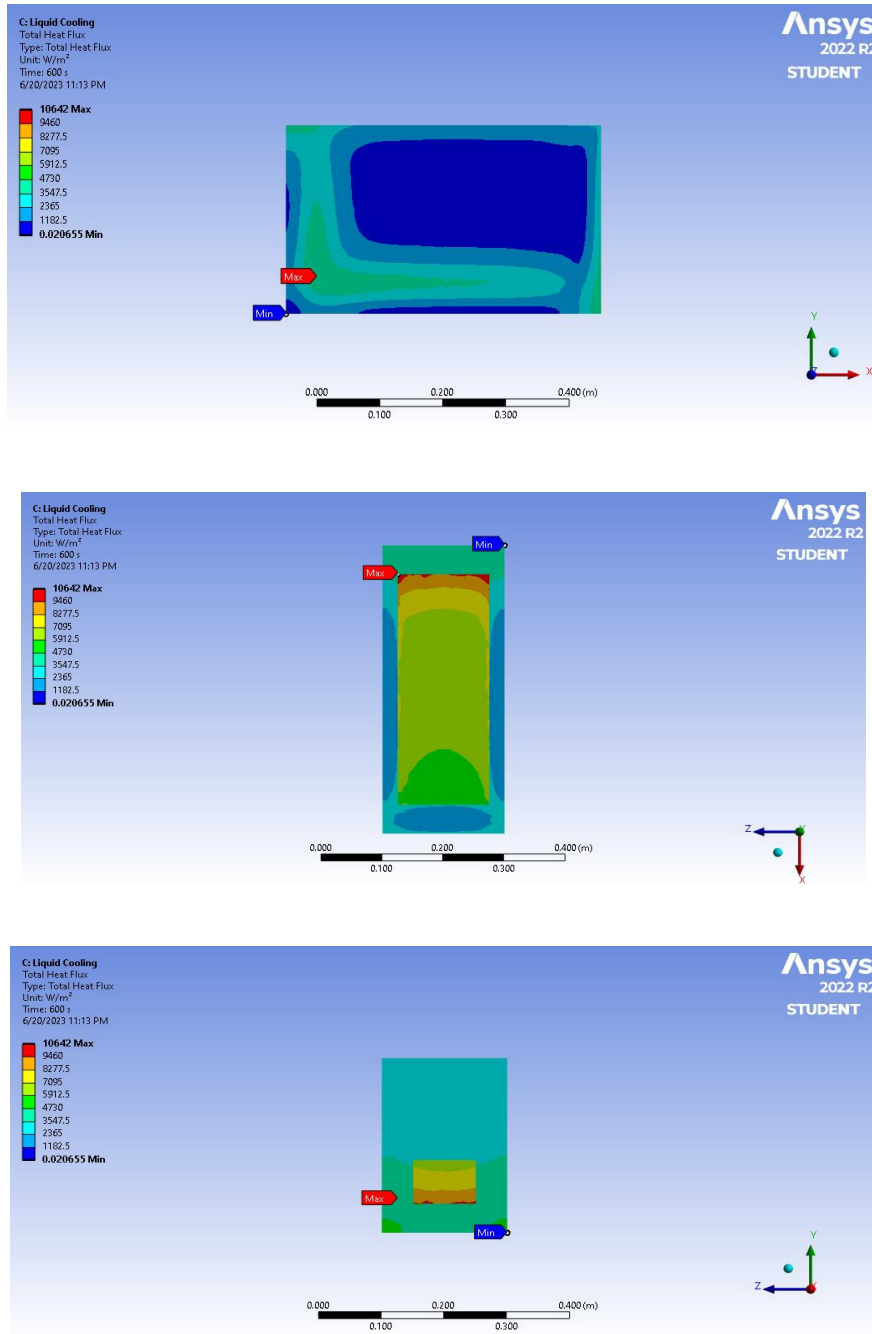
Figure 8. Total Heat Flux Solution of Liquid Cooling

Comparing of Cooling Methods Results from Another Paper Study

Figure 12 presents a bar chart illustrating the minimum and maximum temperature values of each cooling technique. Among the methods examined, fin cooling exhibited the lowest minimum temperature of 20.081 °C. However, in terms of the lowest maximum temperature value, liquid cooling outperformed the other techniques with a value of 34.098 °C. Consequently, these findings indicate that the liquid cooling method is the most suitable option, enabling the battery pack to operate at a lower maximum temperature.
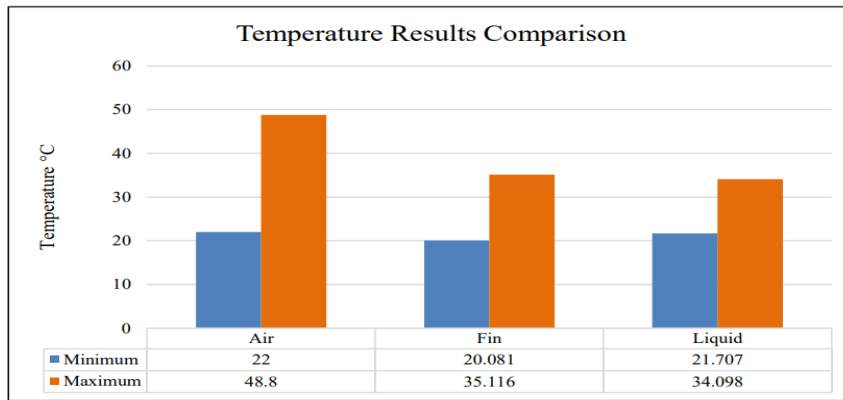
Figure 12. Temperature Results Comparison

PCM Assisted Heat Pipe

Toward the start of the discharging process, PCM which is covered the cell, and the heat pipes warmed up rapidly in conduction mode. The heat pipes quickly get and transfer the heat to the cooling medium (PCM). In the initial process of heat transfer, the heat alongside the heat pipes wall and cell surface is transferred as conduction inside the PCM which is at first in solid state (200 sec). In this stage, the PCM absorbs the heat in sensible form until it arrives at the phase change temperature. Subsequently, a thin axial layer of PCM is melted along the heat pipes and the cell surface as shown at 400 sec. As indicated by the shots, as time passes, heat is dissipated into the PCM, and the melting zone increases (600 sec). As of now the PCM retains the heat as a latent form and in a constant temperature. It is important to take note of that the low thermal conductivity of the PCM has been compensated for by heat pipes. The phase change and temperature contours have been displayed (see Figure 13). The phase change (solid = 0, liquid = 1) is considerably increased as time passes. The phase change is happening in the mushy zone that is in the middle of the solid and liquid parts. Figure shows the temperature distribution of the battery cell installed with heat pipes and PCM. Based on the Figures, the cell temperature for 200 sec, 400 sec, and 600 sec reach 36.27 °C, 48.05 °C, and 54.85 °C respectively. The results show that the battery cell reaches at an appropriately excellent temperature uniformity and maximum temperature utilizing the PCM helped heat pipe cooling system.
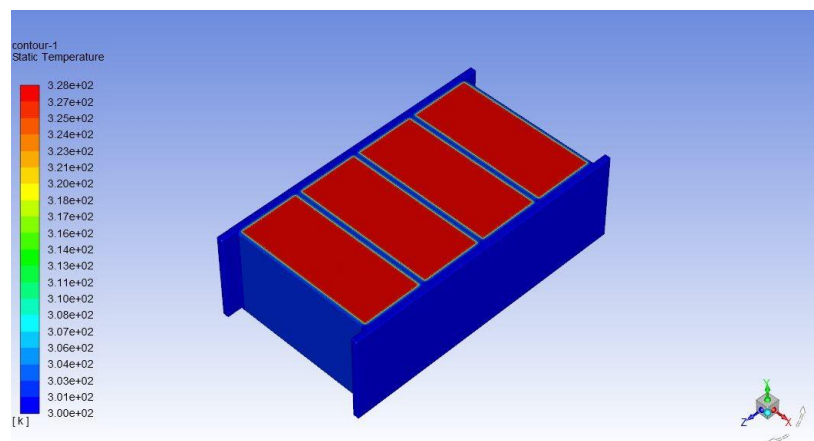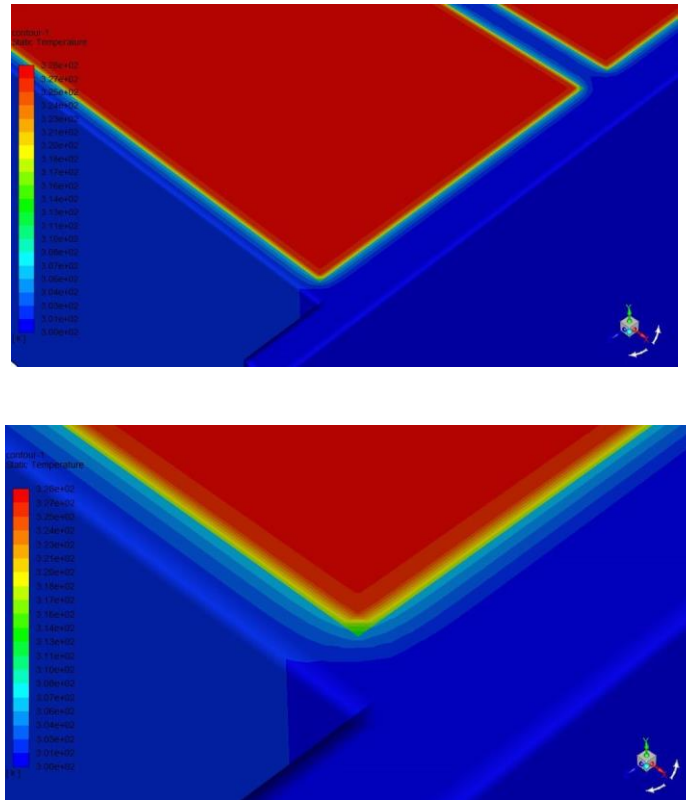
Figure 13. Temperature Solutions for PCM with Heat Pipe

Discussion

Modified Design Improvements

Air outlets were added to a modified battery pack to get the most heat out of it during convection. One outlet was added on the left side. This design improvement was expected to help the total heat flux and temperature arrangements of the air-cooling strategy. The model's internal heat generation rate was 1.1667e+5 W/m^3 with a volume of 0.03 m^3 and a heat rate of 3,500 Watts. The geometry's inlet was subjected to convection at 20 °C with a film coefficient of 1000 W/m^2°C, and the air was uniformly applied to the battery pack's interior walls and top.
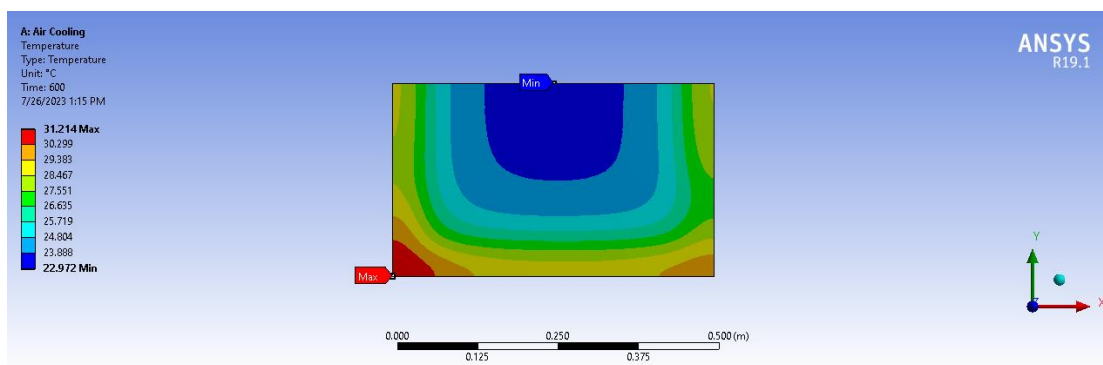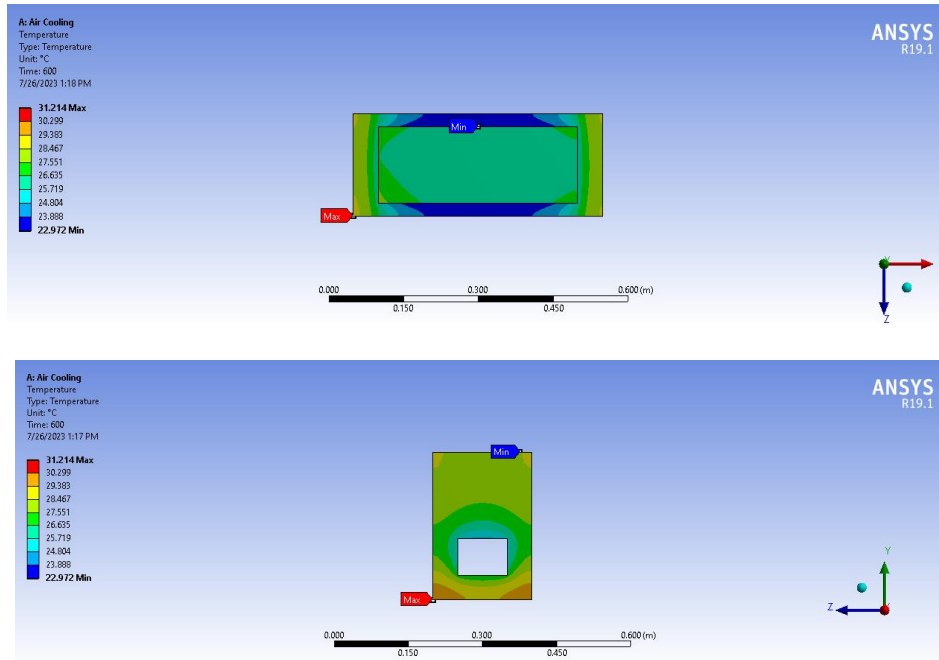
Figure 9. Temperature Solutions for Modified Battery Pack
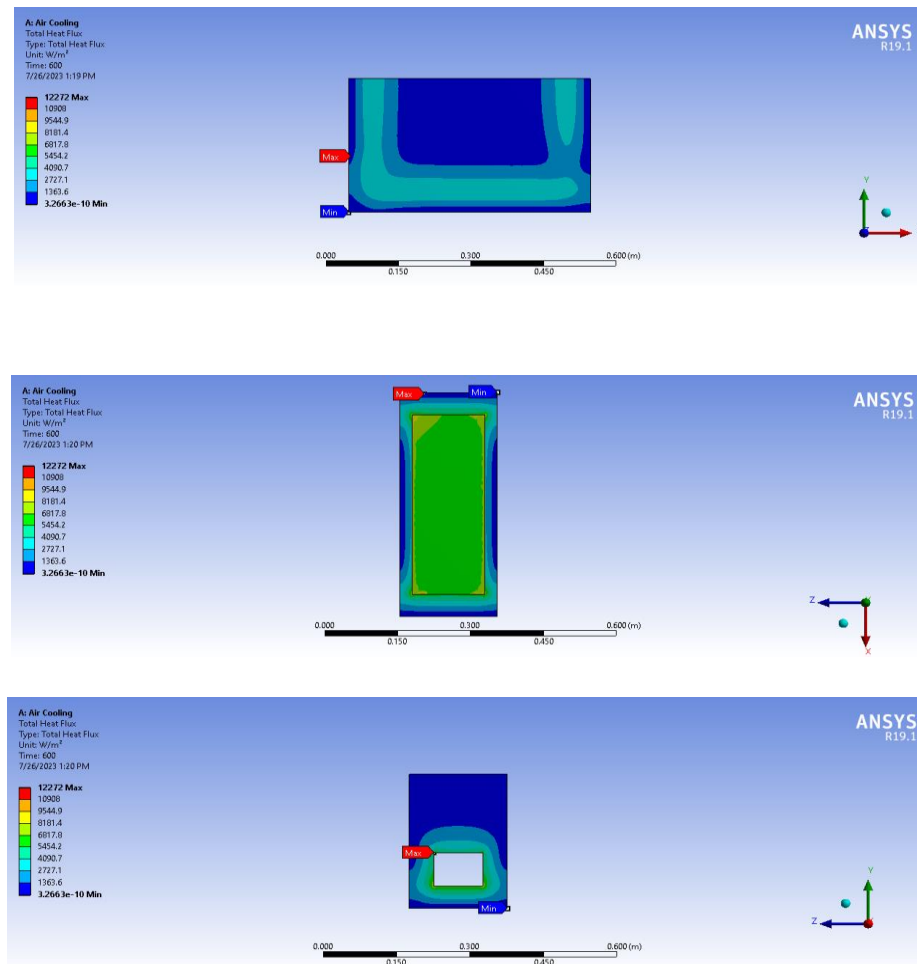
Figure 10. Total Heat Flux Solution for Modified Battery Pack

Figures 9 and 10 depict the temperature distribution at discharge's conclusion for the selected case. demonstrates the effects of air cooling. The temperature gradually rises from the inlet to the outlet in air cooling. Because heat conduction is slower in the bottom layer than it is in the upper layers, the bottom layer is hotter than the upper layers. Due to the relatively low thermal conductive coefficient of air, which is shown by the temperature at the edge of the inlet side, the temperature difference between the surface of the battery pack and the coolant in air cooling is greater than in liquid cooling.

The average temperature of the framework was 26.185 °C, while the minimum temperature was 22.972 °C. This was noticed close to the upper layers and around the outlets where maximum convection was possible. The bottom layer reached its maximum temperature of 31.214 °C due to the battery pack's internal heat, and the simulation result for Total Heat Flux is shown in Figure 10, with the minimum heat flux being 3.2663e-010 W/m^2, the maximum being 12272 W/m^2, and the average being 2924.9 W/m^2. These outcomes depend on a simulation of 600 seconds.

Different Cooling Methods Results Comparison

The Modified Battery Pack's results indicate that this geometry is the most suitable for air-cooling, with air outlets allowing for the lowest maximum temperature value as shown (see Figure 11). With the original geometry, liquid cooling was the best option, but with the new design, air cooling is more effective at maintaining the lowest maximum temperature.

Temperature Results Comparison

	Air	Fin	Liquid	Modified Battery Pack
Minimum	21.754	20.09	21.386	22.972
Maximum	32.928	35.17	31.773	31.214
Average	26.311	23.499	24.746	26.185
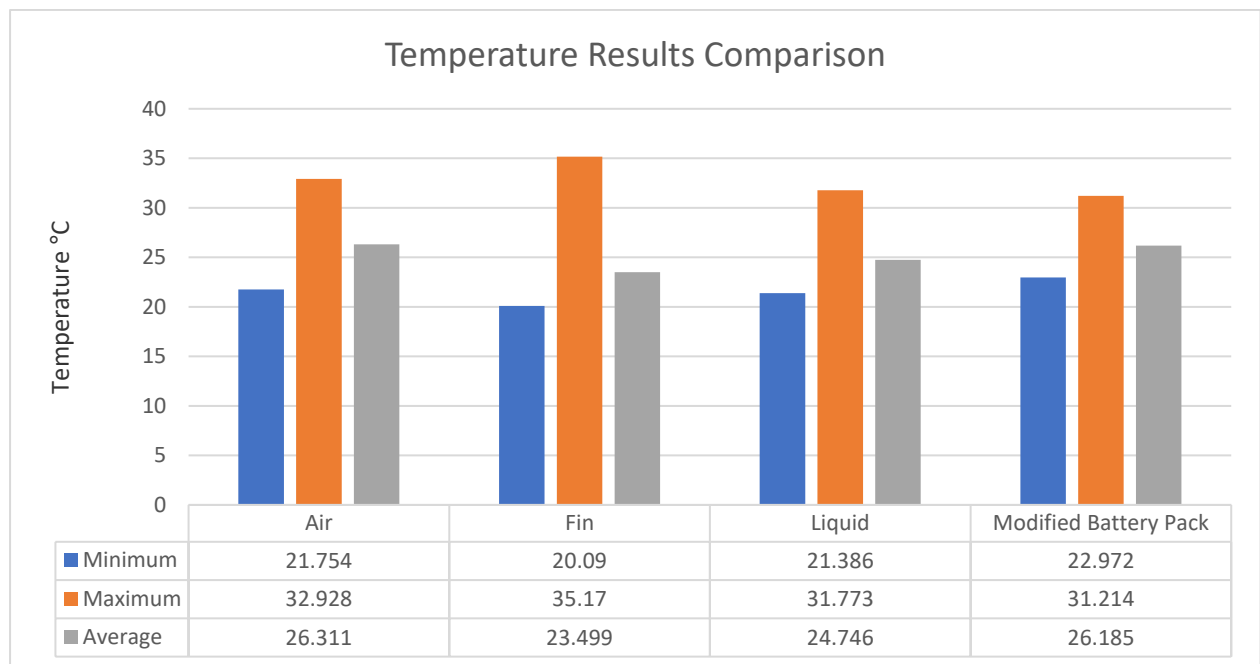
Figure 11. Temperature Comparison with Modified Battery Pack

Conclusion

This paper looked at previous research on cooling methods and the history of lithium-ion batteries. It was suggested that a battery pack with dimensions of 500 x 300 x 200 millimeters be examined. Hypothetical computations of air, liquid, and fin cooling, phase change material cooling (PCM), and heat pipes techniques concluded that the liquid cooling strategy gave the highest heat transfer rate of 4,200 Watts. The initial and final temperatures of 55 °C and 20 °C were used in the calculations. Heat transfer was accomplished by convection in the air and liquid cooling method, and conduction was used to transfer heat in the fin cooling method.

Utilizing ANSYS software to simulate the cooling strategies of lithium-ion batteries was the next phase of the analysis. A geometry of the battery pack was made and afterward meshed to partition it into various areas. The duration of the simulation was set at 600 seconds. The air-cooling technique spreads 20 °C air across the battery pack's top. The Fin cooling technique reproduced 20 °C air on the fin and on the sides of the geometry technique. Results showed that the air-cooling strategy had the highest average heat flux of 3141.5 W/m^2 and the most elevated normal temperature of 26.311 °C. The fin cooling technique had the lowest average temperature at 20.09 °C and the lowest average heat flux at 2379.7 W/m^2. The strategy with the lowest maximum temperature was liquid cooling at 31.773 °C. Additionally, a design enhancement that altered the battery pack was examined. To help remove heat, the proposed design added one air inlets to the battery pack's on the left side. Temperature contours were also obtained by meshing and analyzing this model's geometry in ANSYS. PCM and heat pipe method had a maximum temperature of 54.85 °C and a maximum total heat flow of 554.69 W/m^2. The simulation showed that the liquid cooling encountered the greatest temperature of 31.773 °C, which was the most reduced of all strategies.

Recommendations

An idea for future research is to investigate recycling the heat that is taken out of the lithium-ion battery to heat the vehicle's cabin.

References

Abaza, A.; Ferrari, S.; Wong, H.K.; Lyness, C.; Moore, A.; Weaving, J.; Blanco-Martin, M.; Dashwood, R.; Bhagat, R. (2018, April). Experimental study of internal and external short circuits of commercial automotive pouch lithium-ion cells. *Journal of Energy Storage, 16*, 211–217. https://doi.org/10.1016/j.est.2018.01.015

Al Hallaj, S.; Selman, J.R. (2000). A Novel Thermal Management System for Electric Vehicle Batteries Using Phase-Change Material. *Journal of The Electrochemical Society, 147,* 3231. https://iopscience.iop.org/article/10.1149/1.1393888

Bai, F.; Chen, M.; Song, W.; Feng, Z.; Li, Y.; Ding, Y. (2017, November 5). Thermal management performances of PCM/water cooling-plate using for lithium-ion battery module based on non-uniform internal heat

source. *Applied Thermal Engineering, 126,* 17–27. https://doi.org/10.1016/j.applthermaleng.2017.07.141

Bandhauer, T.M.; Garimella, S.; Fuller, T.F. (2011, January). A critical review of thermal issues in lithium-ion batteries. *Journal of The Electrochemical Society, 158*(3), R1–R25. https://iopscience.iop.org/article/10.1149/1.3515880

Chen, Dafen, et al. (2016, February 5). Comparison of Different Cooling Methods for Lithium Ion Battery Cells. *Applied Thermal Engineering, 94*, 846–854. https://doi.org/10.1016/j.applthermaleng.2015.10.015

Chen, Y., James, W.E. (1994). Three-dimensional thermal modeling of lithium-polymer batteries under galvanostatic discharge and dynamic power profile. *Journal of The Electrochemical Society, 141*(11), 2947 https://iopscience.iop.org/article/10.1149/1.2059263

Choudhari, V.G.; Dhoble, A.S.; Panchal, S. (2020, December). Numerical analysis of different fin structures in phase change material module for battery thermal management system and its optimization. International *Journal of Heat and Mass Transfer, 163*, 120434. https://doi.org/10.1016/j.ijheatmasstransfer.2020.120434

Deng, Y.; Feng, C.; Jiaqiang, E.; Zhu, H.; Chen, J.; Wen, M.; Yin, H. (2018, September). Effects of different coolants and cooling strategies on the cooling performance of the power lithium ion battery system: A review. *Applied Thermal Engineering, 142,* 10–29. https://doi.org/10.1016/j.applthermaleng.2018.06.043

Duan, Yaojuan, et al. (2014). Cooling Simulation and Experimental Analysis on Power Lithium-Ion Battery Pack. *2014 IEEE Conference and Expo Transportation Electrification Asia-Pacific* (ITEC Asia-Pacific), https://doi.org/10.1109/ITEC-AP.2014.6940970

Feng, X.; Pan, Y.; He, X.; Wang, L.; Ouyang, M. (2018, August). Detecting the internal short circuit in large-format lithium-ion battery using model-based fault-diagnosis algorithm. *Journal of Energy Storage, 18,* 26–39. https://doi.org/10.1016/j.est.2018.04.020

Hwang, Hsiu-Ying, et al. (2014, December 23). Optimizing the Heat Dissipation of an Electric Vehicle Battery Pack. *Advances in Mechanical Engineering, 7(*1), 204131. https://doi.org/10.1155/2014/204131

Ismail, Nur Hazima Faezaa, et al. (2013, July). Simplified Heat Generation Model for Lithium Ion Battery Used in Electric Vehicle. *IOP Conference Series: Materials Science and Engineering,* 53, 012014. https://iopscience.iop.org/article/10.1088/1757-899X/53/1/012014

Karimi, G., and X. Li. (2012, January 23). Thermal Management of Lithium-Ion Batteries for Electric Vehicles. *International Journal of Energy Research, 37*(1), 13–24., https://doi.org/10.1002/er.1956

Kim, J.; Oh, J.; Lee, H. (2019, February 25). Review on battery thermal management system for electric vehicles. *Applied Thermal Engineering, 149*, 192–212. https://doi.org/10.1016/j.applthermaleng.2018.12.020

Kokam Co. Ltd. (2016). *KOKAM Li-ion/polymer cell superior lithium polymer battery (SLPB),* pp. 1–5. Kokam Co. Ltd

Li, W.Q., Qu, Z.G., He, Y.L., Tao, Y.B. (2014, June 1). Experimental study of a passive thermal management system for high-powered lithium-ion batteries using porous metal foam saturated with phase change materials. *Journal of Power Sources, 255*, 9–15 https://doi.org/10.1016/j.jpowsour.2014.01.006

Ling, Z., et al. (2014, May 15). Experimental and numerical investigation of the application of phase change materials in a simulative power batteries thermal management system. *Applied Energy, 121*, 104–113 https://doi.org/10.1016/j.apenergy.2014.01.075

Liu, Guangming, et al. (2014, January 31). Analysis of the Heat Generation of Lithium-Ion Battery during Charging and Discharging Considering Different Influencing Factors. *Journal of Thermal Analysis and Calorimetry, 116*(2), 1001–1010. https://link.springer.com/article/10.1007/s10973-013-3599-9

Liu, H.; Wei, Z.; He, W.; Zhao, J. (2017, October 15). Thermal issues about Li-ion batteries and recent progress in battery thermal management systems: A review. *Energy Conversion and Management, 150*, 304–330. https://doi.org/10.1016/j.enconman.2017.08.016

Liu, Yan-Ping, et al. (2015, October 18). Design and Parametric Optimization of Thermal Management of Lithium-Ion Battery Module with Reciprocating Airflow. *Journal of Central South University,22*(10), pp. 3970–3976., https://link.springer.com/article/10.1007/s11771-015-2941-8

Lu, L., Han, X., Li, J., Hua, J., Ouyang, M. (2013, March 15). A review on the key issues for lithium-ion battery management in electric vehicles. *Journal Power Sources, 226,* 272-88. https://doi.org/10.1016/j.jpowsour.2012.10.060

Lv, P.; Liu, C.; Rao, Z. (2017, February). Review on clay mineral-based form-stable phase change materials: Preparation, characterization and applications. *Renewable and Sustainable Energy Reviews, 68,* 707–726. https://doi.org/10.1016/j.rser.2016.10.014

Menale, C.; D'Annibale, F.; Mazzarotta, B.; Bubbico, R. (2019, September 1). Thermal management of lithium-ion batteries: An experimental investigation. *Energy, 182,* 57–71. https://doi.org/10.1016/j.energy.2019.06.017

Mohammadian, S.K., Rassoulinejad-Mousavi, S.M., Zhang, Y. (2015, November 20). Thermal management improvement of an air-cooled high-power lithium-ion battery by embedding metal foam. *Journal of Power Sources 296*, 305–313 https://doi.org/10.1016/j.jpowsour.2015.07.056

Mohammadian, S.K., Zhang, Y. (2015, January 1). Thermal management optimization of an air-cooled Li-ion battery module using pin-fn heat sinks for hybrid electric vehicles. *Journal of Power Sources, 273,* 431–439 https://doi.org/10.1016/j.jpowsour.2014.09.110

Mousavi, Mohsen, et al. (2011). Optimal Design of an Air-Cooling System for a Li-Ion Battery Pack in Electric Vehicles with a Genetic Algorithm. *2011 IEEE Congress of Evolutionary Computation* (CEC), https://doi.org/10.1109/CEC.2011.5949840

Omariba, Z.B.; Zhang, L.; Kang, H.; Sun, D. (2020). Parameter identification and state estimation of lithium-ion batteries for electric vehicles with vibration and temperature dynamics. *World Electric Vehicle Journal, 11*(3), 50. https://doi.org/10.3390/wevj11030050

Park, H. (2013, October 1). A design of air flow configuration for cooling lithium-ion battery in hybrid electric vehicles. *Journal of Power Sources, 239*, 30–36. https://doi.org/10.1016/j.jpowsour.2013.03.102

Pesaran, A.A.; Burch, S.; Keyser, M. (1999, May 24–27). An Approach for Designing Thermal Management Systems for Electric and Hybrid Vehicle Battery Packs. In *Proceedings of the Fourth Vehicle Thermal Management Systems Conference and Exhibition*; London, UK,https://www.researchgate.net/publication/237790937_An_Approach_for_Designing_Thermal_Management_Systems_for_Electric_and_Hybrid_Vehicle_Battery_Packs (accessed on 9 July 2021).

Qian, Z.; Li, Y.; Rao, Z. (2016, October 15). Thermal performance of lithium-ion battery thermal management system by using mini-channel cooling. *Energy Conversion and Management, 126*, 622–631. https://doi.org/10.1016/j.enconman.2016.08.063

Ramadass, P.; Haran, B.; White, R.; Popov, B.N. (2002, November 14). Capacity fade of Sony 18650 cells cycled at elevated temperatures: Part II. Capacity fade analysis. *Journal of Power Sources, 112*, 614–620. https://doi.org/10.1016/S0378-7753(02)00473-1

Rao, Z.; Zhang, X. (2019, May 6). Investigation on thermal management performance of wedge-shaped microchannels for rectangular Li-ion batteries. *International Journal of Energy Research, 43*, 3876–3890. https://doi.org/10.1002/er.4571

Sabbah, R., Kizilel, R., Selman, J.R. (2008, August 1). Active (air-cooled) vs. passive (phase change material) thermal management of high-power lithium-ion packs: limitation of temperature rise and uniformity of temperature distribution. *Journal of Power Sources, 182,* 630–638 https://doi.org/10.1016/j.jpowsour.2008.03.082

Saw, L.h., et al. (2015). Thermal Management of Lithium-Ion Battery Pack with Liquid Cooling. *2015 31st Thermal Measurement, Modeling & Management Symposium* (SEMI-THERM), https://doi.org/10.1109/SEMI-THERM.2015.7100176

Tran, T., Harmand, S., Desmet, B., Filangi, S. (2014, February 22). Experimental investigation on the feasibility of heat pipe cooling for HEV/EV lithium-ion battery. *Applied Thermal Engineering, 63*(2), 551–558. https://doi.org/10.1016/j.applthermaleng.2013.11.048

Tran, T.; Harmand, S.; Desmet, B.; Filangi, S. (2014, February 22). Experimental investigation on the feasibility of heat pipe cooling for HEV/EV lithium-ion battery. *Applied Thermal Engineering, 63*, 551–558. https://doi.org/10.1016/j.applthermaleng.2013.11.048

Wang, Q.; Ping, P.; Zhao, X.; Chu, G.; Sun, J.; Chen, C. (2012, June 15). Thermal runaway caused fire and explosion of lithium-ion battery. *Journal of Power Sources, 208*, 210–224. https://doi.org/10.1016/j.jpowsour.2012.02.038

Wang, Y.-F.; Wu, J.-T. (2020, March 1). Thermal performance predictions for an HFE-7000 direct flow boiling cooled battery thermal management system for electric vehicles. *Energy Conversion and Management, 207*, 112569. https://doi.org/10.1016/j.enconman.2020.112569

Wang, Z., Zhang, Z., Jia, L., Yang, L. (2015, March 5). Parafn and parafn/ aluminum foam composite phase change material heat storage experimental study based on thermal management of Li-ion battery. *Applied Thermal Engineering, 78*, 428–436 https://doi.org/10.1016/j.applthermaleng.2015.01.009

Wei, Y.; Agelin-Chaab, M. (2018, May 25). Experimental investigation of a novel hybrid cooling method for lithium-ion batteries. *Applied Thermal Engineering, 136,* 375–387. https://doi.org/10.1016/j.applthermaleng.2018.03.024

Wu, M.S.; Liu, K.H.; Wang, Y.Y.; Wan, C.C. (2002, June 15). Heat dissipation design for lithium-ion batteries. Journal of Power Sources,109, 160–166. https://doi.org/10.1016/S0378-7753(02)00048-4

Yu, X.; Lu, Z.; Zhang, L.; Wei, L.; Cui, X.; Jin, L. (2019, November). Experimental study on transient thermal characteristics of stagger-arranged lithium-ion battery pack with air cooling strategy. International *Journal of Heat and Mass Transfer, 143,* 118576. https://doi.org/10.1016/j.ijheatmasstransfer.2019.118576

Zhao, W.; Luo, G.; Wang, C.Y. (2015, April 28). Modeling internal shorting process in large-format Li-ion cells. *Journal of The Electrochemical Society, 162,* A1352–A1364. https://iopscience.iop.org/article/10.1149/2.1031507jes

Zhou, L.; Zheng, Y.; Ouyang, M.; Lu, L. (2017, October 1). A study on parameter variation effects on battery packs for electric vehicles. *Journal of Power Sources, 364,* 242–252. https://doi.org/10.1016/j.jpowsour.2017.08.033

Author Information

Amany Belal

 https://orcid.org/0009-0003-2788-0220

Arab Academy for Science and Technology and Maritime Transport (AASTMT).

1029 Abu Kir, Alexandria.

Egypt

Contact e-mail:

engineer.amanymahmoud@gmail.com

Ali I. Shehata

 https://orcid.org/0000-0003-2174-7368

Mechanical Engineering Department, College of Engineering and Technology, Arab Academy of Science, Technology and Maritime Transport (AASTMT).

1029 Abu Kir, Alexandria.

Egypt

Yehia A. Eldrainy

 https://orcid.org/0000-0001-9646-3365

Mechanical Engineering Department, College of Engineering and Technology, Arab Academy of Science, Technology and Maritime Transport (AASTMT).

1029 Abu Kir, Alexandria.

Egypt

Essam H. Seddik

 https://orcid.org/0000-0002-9987-0385

Mechanical Engineering Department, College of Engineering and Technology, Arab Academy of Science, Technology and Maritime Transport (AASTMT).

1029 Abu Kir, Alexandria.

Egypt